Title
Quantification of Holocene Asian monsoon rainfall from spatially separated cave records

Journal
Earth and Planetary Science Letters, 266(3-4)

ISSN
0012-821X

Authors
Hu, Chaoyong
Henderson, Gideon M
Huang, Junhua
et al.

Publication Date
2008-02-01

DOI
10.1016/j.epsl.2007.10.015

Available online at www.sciencedirect.com
ScienceDirect
Earth and Planetary Science Letters 266 (2008) 221–232
EPSL
www.elsevier.com/locate/epsl

Quantification of Holocene Asian monsoon rainfall from spatially separated cave records

Chaoyong Hu [a], Gideon M. Henderson [b,*], Junhua Huang [a,c], Shucheng Xie [a,c], Ying Sun [d], Kathleen R. Johnson [b]

[a] *Key Laboratory of Biogeology and Environmental Geology, Ministry of Education, China University of Geosciences, Wuhan, 430074, PR China*
[b] *Department of Earth Sciences, University of Oxford, Oxford, OX1 3 PR, UK*
[c] *State Key Laboratory of Geological Processes and Mineral Resources, China University of Geosciences, Wuhan, 430074, PR China*
[d] *National Climate Center, Beijing, 100081, PR China*

Received 20 June 2007; received in revised form 24 August 2007; accepted 2 October 2007
Available online 14 October 2007
Editor: H. Elderfield

Abstract

A reconstruction of Holocene rainfall is presented for southwest China — an area prone to drought and flooding due to variability in the East Asian monsoon. The reconstruction is derived by comparing a new high-resolution stalagmite $\delta^{18}O$ record with an existing record from the same moisture transport pathway. The new record is from Heshang Cave (30°27′N, 110°25′E; 294 m) and shows no sign of kinetic or evaporative effects so can be reliably interpreted as a record of local rainfall composition and temperature. Heshang lies 600 km downwind from Dongge Cave which has a published high-resolution $\delta^{18}O$ record (Wang, Y.J., Cheng, H., Edwards, R.L., He, Y.Q., Kong, X.G., An, Z.S., Wu, J.Y., Kelly, M.J., Dykoski, C.A., Li, X.D., 2005. The Holocene Asian monsoon: links to solar changes and North Atlantic climate. Science 308, 854–857). By differencing co-eval $\delta^{18}O$ values for the two caves, secondary controls on $\delta^{18}O$ (e.g. moisture source, moisture transport, non-local rainfall, temperature) are circumvented and the resulting $\Delta\delta^{18}O$ signal is controlled directly by the amount of rain falling between the two sites. This is confirmed by comparison with rainfall data from the instrumental record, which also allows a calibration of the $\Delta\delta^{18}O$ proxy. The calibrated $\Delta\delta^{18}O$ record provides a quantitative history of rainfall in southwest China which demonstrates that rainfall was 8% higher than today during the Holocene climatic optimum (≈6 ka), but only 3% higher during the early Holocene. Significant multi-centennial variability also occurred, with notable dry periods at 8.2 ka, 4.8–4.1 ka, 3.7–3.1 ka, 1.4–1.0 ka and during the Little Ice Age. This Holocene rainfall record provides a good target with which to test climate models. The approach used here, of combining stalagmite records from more than one location, will also allow quantification of rainfall patterns for past times in other regions.

Keywords: East Asian monsoon; speleothem; paleoclimate; rainfall

1. Introduction

Rainfall has an obvious importance for terrestrial eco systems and human societies but is difficult to predict

* Corresponding author. Tel.: +44 1865 282123; fax: +44 1865 272072.
E-mail address: gideonh@earth.ox.ac.uk (G.M. Henderson).

0012-821X/$ - see front matter © 2008 Published by Elsevier B.V.
doi:10.1016/j.epsl.2007.10.015

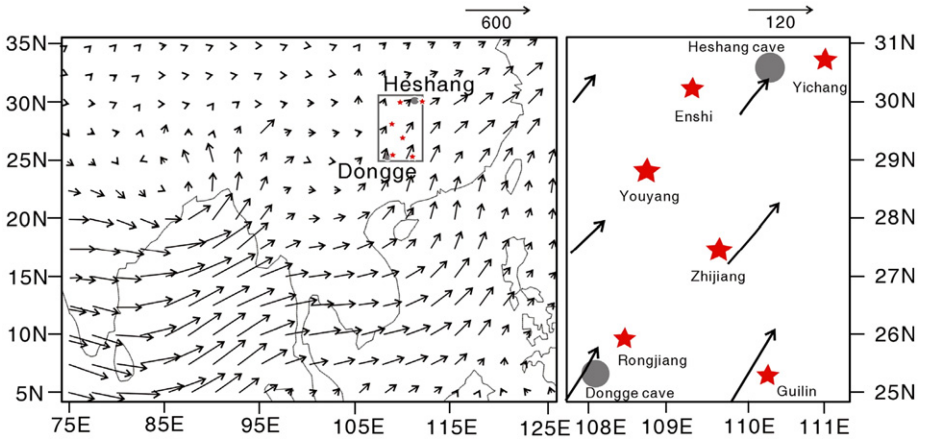

Fig. 1. Map showing the location of Heshang cave (this study) and Dongge cave (Wang et al., 2005). Arrows show the average total-column moisture transport for June–July–August (Ding et al., 2004) in kg m^{-1} s^{-1}. These values are based on reanalysis of modern atmospheric measurements and are derived by multiplying humidity (kg/m^3) by wind speed (m/s) and summing over the whole air column. The box indicates the specific region for which comparison of Heshang and Dongge allows rainfall reconstruction, and the red stars show the location of six modern rainfall stations (Enshi, Yichang, Youyang, Zhijiang, Rongjiang, and Guilin).

with present climate models. Quantitative records of past rainfall, which extend the relatively short instrumental record, would offer significant insight into natural rainfall variability and the pattern of rainfall under different climate states. Such records are particularly important for regions impacted by major and potentially variable climate systems such as the Asian monsoon, a region where prediction of future rainfall is difficult (IPCC, 2007).

Stalagmites can provide precisely-dated records of $\delta^{18}O$ — a geochemical proxy that, in regions dominated by atmospheric convection, is strongly influenced by the amount of rainfall (Dansgaard, 1964). Several high-resolution $\delta^{18}O$ records have recently been published from such regions including China (Wang et al., 2005, 2001; Dykoski et al., 2005), Oman (Burns et al., 2003; Fleitmann et al., 2003), and Brazil (Wang et al., 2004). Such records from the region impacted by the East Asian monsoon indicate dramatic changes of rainfall associated with cool events in the North Atlantic region (Wang et al., 2001) and the possible influence of solar variation in controlling monsoon strength (Wang et al., 2005).

Converting stalagmite $\delta^{18}O$ records into a quantitative assessment of past rainfall amount is difficult, however, because $\delta^{18}O$ in cave carbonates is also controlled by other environmental variables (Bar-Matthews et al., 1999; McDermott, 2004) including cave temperature, local evaporation, the $\delta^{18}O$ of the source, and the transport distance from the source. In the Asian monsoon region, for instance, although rainfall amount is thought to be the dominant control on stalagmite $\delta^{18}O$ (Johnson and Ingram, 2004) and high quality $\delta^{18}O$ records exist e.g. (Wang et al., 2005; Fleitmann et al., 2003), converting these records into a quantitative assessment of past rainfall is uncertain and has not been performed. In addition, a single record of $\delta^{18}O$ provides no information about the location of the rainfall. Rainfall $\delta^{18}O$ reflects the total moisture loss along the atmospheric transport path so, in regions where transport distances are long, rainfall variability a considerable distance from the measurement site might control the

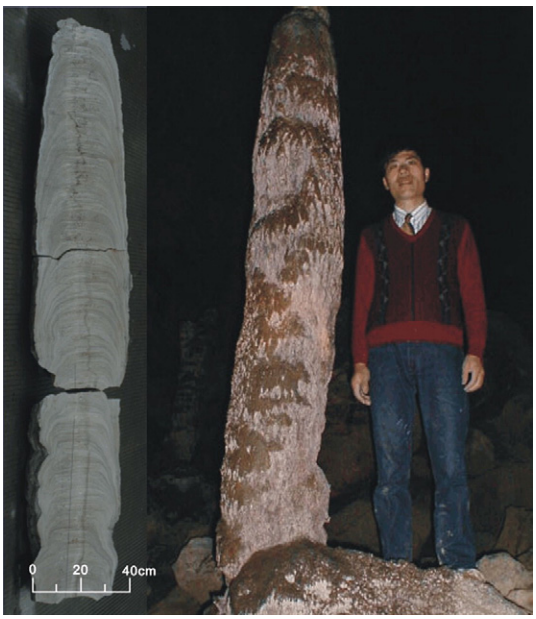

Fig. 2. A photograph of the complete HS-4 sample in the lab (left) and in the field with the first author for scale (right). The track of $\delta^{18}O$ sampling is just visible running along the centre of the stalagmite in the left-hand figure.

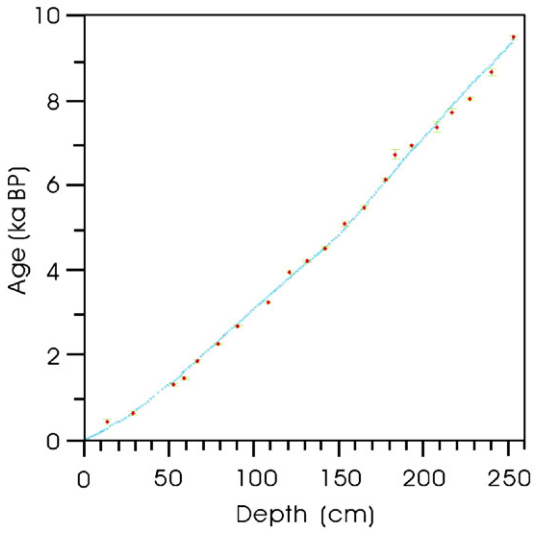

Fig. 3. U/Th and layer counting chronologies for stalagmite HS-4. Red data points are U/Th ages with 2σ uncertainties (Table 1). The blue line represents layer-counting chronology and is in close agreement with the U/Th dates.

measured δ^{18}O signal. This inability to quantify rainfall amount or location from speleothem records represents a significant limitation on the use of these otherwise powerful archives of high-resolution paleoclimate.

In this paper we present a new approach to allow quantification of rainfall by comparing stalagmite δ^{18}O records from two caves along the same moisture transport path. We use this approach to quantify the history of rainfall in southwest China during the Holocene by comparing a new precisely-dated stalagmite δ^{18}O record described below with a published record (Wang et al., 2005). This is a region prone to flooding when monsoon rainfall is strong (part of the motivation for the recent construction of the Three Gorges Dam in the region) so understanding the amplitude of rainfall variation in this area has a particular societal importance.

2. Samples and location

Heshang Cave is situated in the Qingjiang Valley of the middle reaches of the Yangtze River (30°27′N, 110°25′E; 294 m) (Fig. 1). Annual climate in this region is strongly monsoonal. In the boreal summer, average temperatures of 28 °C drive convection, drawing moist air from the south to generate rainfall peaking in July at 270 mm/month. In the boreal winter, temperature drops below 10 °C, air movement is from the north, and rainfall is less than 50 mm/month.

Heshang Cave is approximately horizontal and extends a distance of ≈250 m backwards from its reasonably large opening. It is overlain by ≈400 m of Cambrian dolomite with recharge therefore occurring at an altitude of ≈650 m. The cave is well decorated with stalagmites, rimstone pools, and less frequent stalactites. Three samples have been recovered, all from a distance of ≈150 m within the cave: HS-2 (Hu et al., 2005); HS-4 (the main focus of this study); and HS-6 (from which limited results are also presented here). Stalagmite HS-4 is 2.5 m long (Fig. 2) and was actively growing when recovered from Heshang Cave in 2001. It shows clear annual banding throughout its length, generated by the strong seasonal cycle at this site, and associated with geochemical signals which are the focus of ongoing efforts to reconstruct past climate at seasonal resolution (Johnson et al., 2006). Such seasonal variations are averaged out at the resolution of measurement presented in this paper.

3. Chronology and analytical techniques

The chronology of stalagmite HS-4 has been established independently by U–Th dating and layer counting. For U/Th analysis, 21 samples of ≈1 g of stalagmite calcite were dissolved, spiked with a mixed ^{229}Th–^{236}U spike, purified by ion-exchange chemistry, and analysed by multi-collector ICP mass spectrometer at Oxford (Nu Instruments). Techniques broadly followed those used for other carbonate samples at Oxford (Robinson et al., 2002). Samples were handled in a class-1000 clean lab and chemical blanks, although corrected for, were insignificant.

U/Th ages are corrected for the presence of small amounts of initial Th using a (^{230}Th/^{232}Th) ratio (where round brackets signify activity ratio) measured directly on the drip waters that formed HS-4. A beaker was placed under the drip for some days, during which time the water it collected degassed and precipitated calcite which could readily be recovered for analysis. This collection technique is reasonably analogous to the growth of stalagmite calcite and gives an accurate assessment of the modern day (^{230}Th/^{232}Th) value captured by HS-4. The measured value (1.97) is higher than typical crustal values (≈1.0), indicating the addition of ^{230}Th from the overlying dolomite and requiring a somewhat larger age correction for a given ^{232}Th concentration. Age corrections are made using this ratio and the measured ^{232}Th for each sample. They average 112 yrs and, with an assumed 50% uncertainty, dominate final age uncertainties which average 67 yrs.

Stable isotope samples were drilled continuously from the entire length of HS-4. A total of 1223 samples were measured on a Finnegan MAT 251 instrument at Wuhan, China with a precision of 0.1‰ (based on long-term repeatability of standard measurements). These

Table 1
U and Th concentrations and isotope ratios with resulting U–Th ages

Distance (cm)	^{238}U conc (ppm)	^{232}Th conc (ppb)	δ^{234}U [a]	(^{230}Th/^{232}Th) [b]	(^{230}Th/^{238}Th) [b]	Age (raw) [c] (yrs BP)	Age (corr) [d] (yrs BP)
13.0	0.4657± 0.0015	1.277± 0.014	747.9± 2.9	10.9± 0.3	0.0087± 0.0002	489± 13	378± 57
28.6	0.4164± 0.0005	1.450± 0.001	796.3± 2.3	11.8± 0.1	0.0130± 0.0002	740± 10	603± 69
53.0	0.4875± 0.0006	1.427± 0.001	816.1± 2.3	25.0± 0.2	0.0238± 0.0002	1387± 13	1273± 59
59.0	0.5091± 0.0006	1.500± 0.002	836.9± 2.3	27.7± 0.1	0.0267± 0.0002	1542± 12	1427± 58
67.0	0.6066± 0.0007	2.298± 0.005	824.3± 2.3	27.0± 0.1	0.0335± 0.0002	1966± 13	1818± 75
79.0	0.4982± 0.0006	0.792± 0.001	834.3± 2.3	73.5± 0.4	0.0389± 0.0002	2286± 15	2224± 34
91.0	0.5458± 0.0007	0.973± 0.001	819.0± 2.3	76.9± 0.3	0.0457± 0.0002	2722± 15	2651± 38
109.0	0.6903± 0.0008	2.003± 0.003	793.6± 2.3	57.4± 0.3	0.0548± 0.0003	3328± 17	3211± 61
121.0	0.5561± 0.0007	1.734± 0.002	848.5± 2.3	66.1± 0.2	0.0681± 0.0002	4038± 15	3915± 63
131.0	0.4894± 0.0006	0.496± 0.001	872.5± 2.3	207.1± 0.8	0.0721± 0.0003	4221± 20	4181± 28
142.0	0.4846± 0.0006	1.423± 0.002	821.1± 2.3	78.0± 0.2	0.0761± 0.0003	4591± 19	4474± 62
154.0	0.4803± 0.0006	2.134± 0.004	814.7± 2.3	58.9± 0.3	0.0863± 0.0005	5251± 33	5071± 95
165.8	0.5586± 0.0018	0.591± 0.003	838.5± 2.9	273.8± 1.5	0.0912± 0.0007	5485± 46	5443± 50
177.0	0.4654± 0.0006	0.973± 0.001	826.8± 2.3	145.8± 0.3	0.1018± 0.0003	6182± 19	6098± 46
183.6	0.5177± 0.0016	0.714± 0.004	811.2± 2.9	249.4± 2.6	0.1100± 0.0016	6756± 102	6699± 106
193.0	0.4096± 0.0005	0.435± 0.000	767.1± 2.3	299.3± 0.9	0.1099± 0.0004	6929± 29	6884± 36
208.0	0.4241± 0.0005	3.892± 0.006	741.0± 2.3	40.0± 0.1	0.1204± 0.0004	7733± 25	7339± 198
217.0	0.4054± 0.0005	1.778± 0.003	737.1± 2.3	84.6± 0.3	0.1226± 0.0005	7899± 34	7710± 100
228.0	0.4468± 0.0005	0.908± 0.001	733.4± 2.3	182.9± 0.4	0.1249± 0.0003	8071± 25	7983± 51
240.0	0.4434± 0.0014	0.964± 0.007	795.3± 2.9	204.2± 1.2	0.1393± 0.0010	8719± 63	8627± 78
253.0	3.7968± 0.0119	3.127± 0.052	710.9± 2.9	555.6± 1.1	0.1439± 0.0006	9483± 43	9446± 46

All errors are 2σ. Distance is from top of stalagmite HS-4.
[a] $\delta^{234}U=[(^{234}U/^{238}U)-1]\cdot 1000$ where (^{234}U/^{238}U) is the measured activity ratio.
[b] Round brackets signify activity ratios.
[c] Age is calculated using half lives from (Cheng et al., 2000) and is quoted relative to 1950. Uncertainties incorporates mass spectrometric uncertainty, weighing uncertainty, and spike uncertainty.
[d] Raw ages are corrected for initial ^{230}Th content using the measured ^{232}Th content and assuming an initial (^{230}Th/^{232}Th)=1.97 (a value based on a measurement of the present-day drip water chemistry). Uncertainty in this correction is assumed to be 50% of the size of the correction.

have a resolution of ≈2 yrs in the uppermost 2000 yrs and, on average, 16 yrs in the rest of the record. In addition to these growth-axis samples, samples were taken from HS-4 along growth layers at each of two depths (≈173 cm and ≈216 cm). These samples were analysed for stable isotopes to assess the presence of possible kinetic effects during stalagmite growth (i.e. a Hendy test, (1971)). A total of 105 samples were also analysed from the top of a second stalagmite (HS-6) to assess whether the HS-4 record is representative of the Heshang environment.

4. Results

U/Th ages increase systematically with depth to 9.45 ka (all ages are quoted relative to 1950) at the base of HS-4, (Table 1, Fig. 3) and indicate an approximately constant growth rate averaging 270 μm per year. The layer-counting chronology is in broad agreement (Fig. 3), indicating clearly that the lamina in HS-4 are annual. Over short periods the layer counting chronology is likely to be more precise than the U/Th chronology, but cumulative errors and subjectivity in counting make the U/Th chronology more accurate over longer time periods. We therefore use the U/Th chronology for this study except for the uppermost 150 yrs of the stalagmite where layer counting provides better precision. The most significant deviation between the two chronologies occurs at ≈6–7 ka, a period where chronological uncertainty would not cause any change to the interpretation presented here. A smaller deviation between the chronologies at ≈8 ka would make events at this period about 100 yrs older if the layer counting chronology was used in place of the U/Th chronology. The age model beyond 150 yrs is derived by simple linear interpolation between U/Th ages.

Oxygen isotope values range from −10.6 to −7.3‰ (relative to the V-PDB standard) with low values during the early Holocene (≈9 to 5 kyr) and higher values more recently (Fig. 4). Some millennial structure is apparent, with high δ^{18}O intervals at around 3.3, 4.3 and 8.2 kyr. Carbon isotope values are reasonably constant at −11‰, with millennial structure most apparent as two excursions to higher values at 7.3 and 8.2 ka (Fig. 4). There is

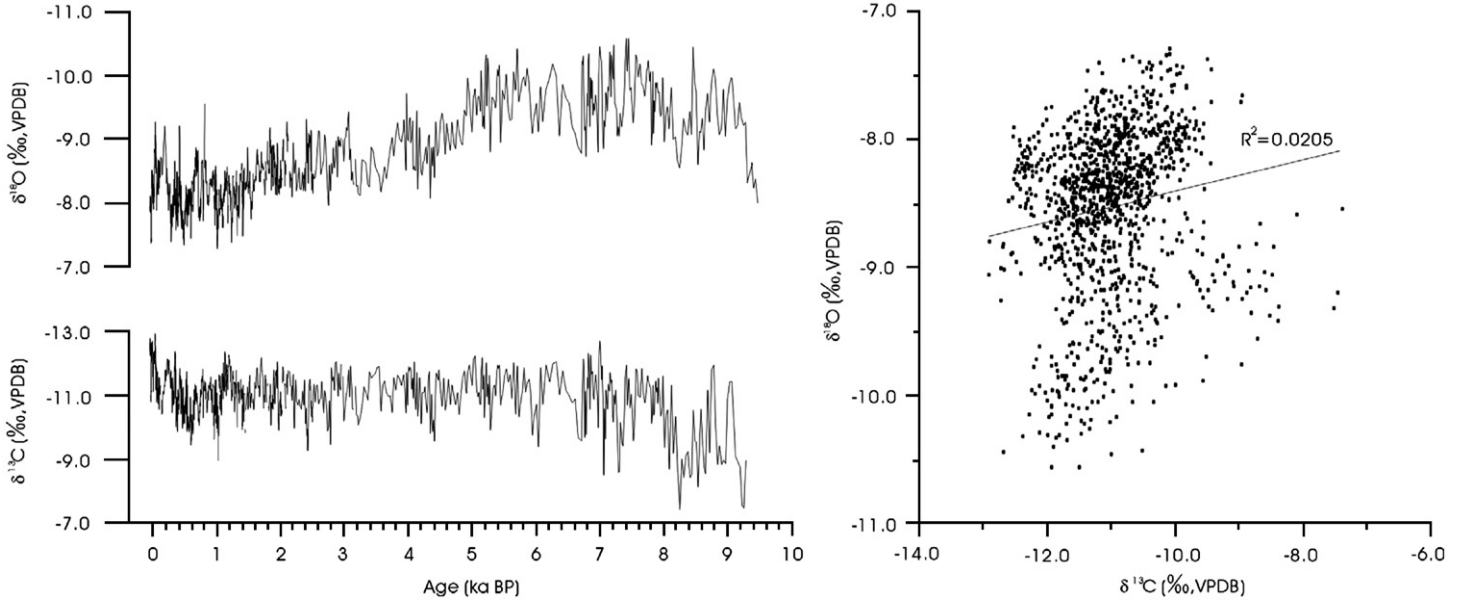

Fig. 4. $\delta^{18}O$ and $\delta^{13}C$ for HS-4 and a cross plot of $\delta^{18}O$ versus $\delta^{13}C$. The latter demonstrates the lack of a relationship between the two isotope systems, suggesting the absence of any kinetic control on isotope fractionation during stalagmite growth. The full dataset is available at the NOAA National Geophysical Data Centre.

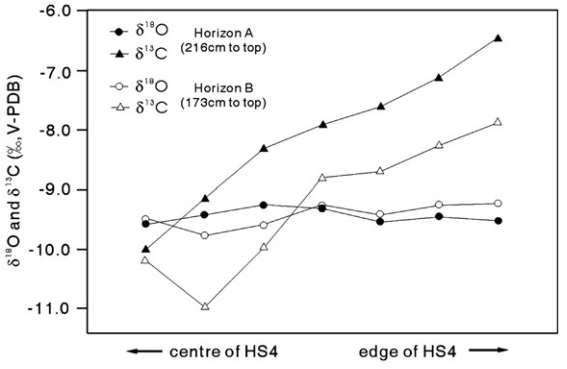

Fig. 5. $\delta^{18}O$ and $\delta^{13}C$ analysis from two horizons in HS-4 taken from the centre to the edge of the stalagmite. Carbon isotopes become progressively heavier towards the edge due to degassing of isotopically light CO_2 as waters flow over the surface. Oxygen isotopes show no systematic trend indicating that there is sufficient time for isotopic equilibration with oxygen in the water as the carbonate forms. HS-4 therefore passes the "Hendy test" (Hendy, 1971).

no correlation between $\delta^{18}O$ and $\delta^{13}C$ (Fig. 4). Samples drilled from single layers in HS-4 show significant increases in $\delta^{13}C$ (by up to 4‰) towards the edge of the sample, but approximately constant $\delta^{18}O$ values with no indication of a systematic trend with distance from the centre of the stalagmite (Fig. 5). The oxygen isotope composition of samples from the upper section of HS-6 agree very closely with those from HS-4 (Fig. 6).

5. Discussion

5.1. Confirmation of isotope equilibrium

If calcite precipitation is rapid during stalagmite growth there can be insufficient time for oxygen isotopes to equilibrate between water and the bicarbonate ion (Hendy, 1971). This leads to Rayleigh fractionation processes in the bicarbonate reservoir and generates systematic increases in $\delta^{18}O$ which have no direct relationship to $\delta^{18}O$ of dripwater or to cave temperature. Such kinetic effects at best complicate, and in most cases prevent, the use of stalagmites for climate reconstruction. It is therefore important to assess whether stalagmite growth has occurred in equilibrium conditions before interpreting $\delta^{18}O$ records for paleoclimate. Four lines of evidence indicate that $\delta^{18}O$ in HS-4 formed in equilibrium with the dripwaters in Heshang Cave:

i. Recently formed carbonate has a $\delta^{18}O$ value identical to that predicted from equilibrium (Kim and O'Neil, 1997), given weighted-average drip-water $\delta^{18}O$ of −7.4 and an annual average cave temperature of 17.1 °C (Johnson et al., 2006).

ii. There is no correlation between $\delta^{13}C$ and $\delta^{18}O$ in the Holocene record (Fig. 3). Kinetic effects leads to such correlation (Hendy, 1971) and, although there are other ways to generate such a correlation in a stalagmite time-series, its absence from the HS-4 record indicates the lack of any kinetic effect.

iii. $\delta^{18}O$ in the upper section of two Heshang stalagmite is identical (Fig. 6) which is difficult to explain unless precipitation is at equilibrium in both records.

iv. $\delta^{18}O$ is uniform within each of two growth band in HS-4. Progressive degassing and calcite precipitation leads to a systematic $\delta^{13}C$ increase as drip waters flows over the surface of the stalagmite. In the absence of kinetic effects, this $\delta^{13}C$ increase will not be accompanied by changes in $\delta^{18}O$, because an insignificant proportion of the oxygen present in the water is precipitated as calcite. HS-4 passes this "Hendy test" (Hendy, 1971).

The absence of any indication of kinetic effects indicate that the HS-4 $\delta^{18}O$ record is a function only of dripwater $\delta^{18}O$ and cave temperature. Modern dripwaters in the cave have a weighted average $\delta^{18}O$ of −7.4 (Johnson et al., 2006) identical to that expected for average rainfall at the location based on modelling of rainfall data (Bowen and Revenaugh, 2003), indicating that evaporation does not alter the $\delta^{18}O$ of rainwater before it precipitates carbonate. This is not surprising because recharge into Heshang cave is rapid, and because the cave is wet throughout the year with measured humidity levels always close to 100%. The HS-4 record can therefore be interpreted as a function only of local rainwater $\delta^{18}O$ and cave temperature.

5.2. Isolating rainfall information by comparison of $\delta^{18}O$ at two sites

In common with other records of the East Asian monsoon (e.g. Wang et al., 2005) $\delta^{18}O$ in the HS-4 stalagmite is low during the early Holocene and increases during the mid Holocene with superimposed millennial and centennial variability (Fig. 4). Such $\delta^{18}O$ changes have generally been interpreted as reflecting higher rainfall during the mid Holocene. Most simply, moisture from a single southerly source becomes progressively lighter as rainfall amount increases due to Rayleigh fractionation and evaporative effects in the atmosphere (Dansgaard, 1964). Other controls also influence stalagmite $\delta^{18}O$, however, and most be considered before records can be interpreted as rainfall amount. Temperature is likely to co-vary with monsoon

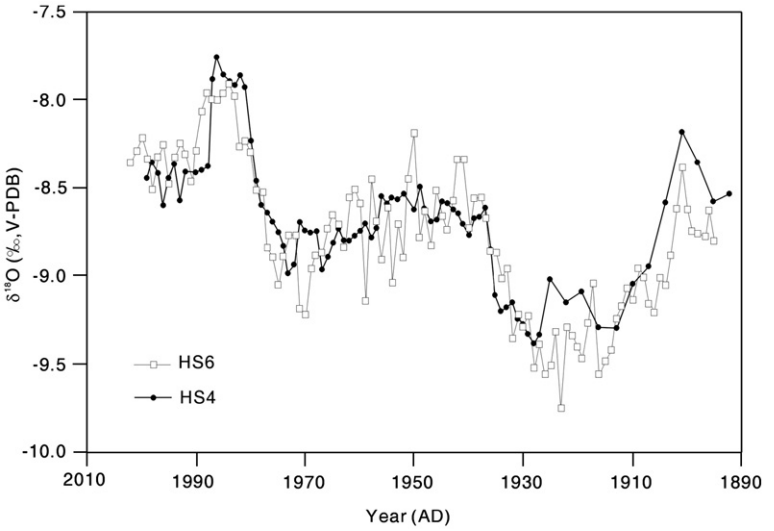

Fig. 6. $\delta^{18}O$ records from the upper 110 yrs of two stalagmites from Heshang Cave showing excellent agreement, suggesting the lack of kinetic or stalagmite-specific overprints on the climate signal.

strength and will influence the size of the isotope fractionation imposed during carbonate growth. Similarly, $\delta^{18}O$ in the source region may change with time, or the location of this source may move. Additionally, increased rainfall upwind of Heshang Cave, in the South China Sea for instance, could lead to low $\delta^{18}O$ in southwest China even if local rainfall actually decreased. This is a significant point because the East Asian monsoon is not characterized by a uniform change in conditions, but rather by changes in the distribution of rainfall along the moisture transport pathway from sea to land (Wang, 2002; Ding et al., 2004).

These secondary controls can, however, be removed from the $\delta^{18}O$ record by comparing $\delta^{18}O$ from two stalagmites growing along the same atmospheric moisture transport pathway. As long as both stalagmites grew without kinetic or evaporative modification of their $\delta^{18}O$ signals, then the difference between $\delta^{18}O$ at the two sites only reflects loss of moisture from the atmosphere by rainfall as the air travels between them. The magnitude of the difference in $\delta^{18}O$ between the two sites reflects the amount of rain removed. Source-water $\delta^{18}O$; the location of the source; and the amount of rainfall since leaving the source may all influence $\delta^{18}O$ at both locations, but will not influence the difference between the two stations. If the two caves are reasonably close to one another they will also have a similar temperature history so changes in temperature will also not influence the difference in $\delta^{18}O$ between the two sites. A caveat to this approach is that the altitude of the cave recharge must be similar at the two sites or, if different, must be corrected for (because increasing altitude causes systematic lightening of rainfall $\delta^{18}O$) but this can readily be achieved.

In this study we have followed this approach by comparing our new Holocene $\delta^{18}O$ record with a published record from Dongge Cave (25°17′N, 108°5′E). Dongge Cave lies 600 km SW of Heshang, directly upstream along the atmospheric pathway by which moisture arrives at Heshang during the summer monsoon (Fig. 1). Winter moisture transport is broadly the reverse of this summer transport, but less than 20% of annual rainfall falls in the winter so rainfall (and therefore stalagmite) $\delta^{18}O$ is dominated by the summer monsoon. There are two published Holocene $\delta^{18}O$ records from Dongge (Wang et al., 2005; Dykoski et al., 2005) which show some differences in detail but which, overall, have similar structure. Here we focus on the record from stalagmite DA (Wang et al., 2005) which is at higher resolution and features a more uniform growth rate. The same analysis performed with stalagmite D4 (Dykoski et al., 2005) supports the interpretation presented below. The $\delta^{18}O$ record of Heshang and Dongge show some similarity of structure, reflecting their location in the same climate system. A plot of fifty year averages of $\delta^{18}O$ has an r^2 of 0.78 indicating that much, though not all, of the variability in the two records is common.

As expected for a site further along the moisture transport pathway, speleothem $\delta^{18}O$ at Heshang is lower than at Dongge throughout the Holocene (Fig. 7). The average difference is 1.0‰, of which less than a third can be explained by the small (1.5 °C) temperature difference between the two caves. The altitude of recharge at the two

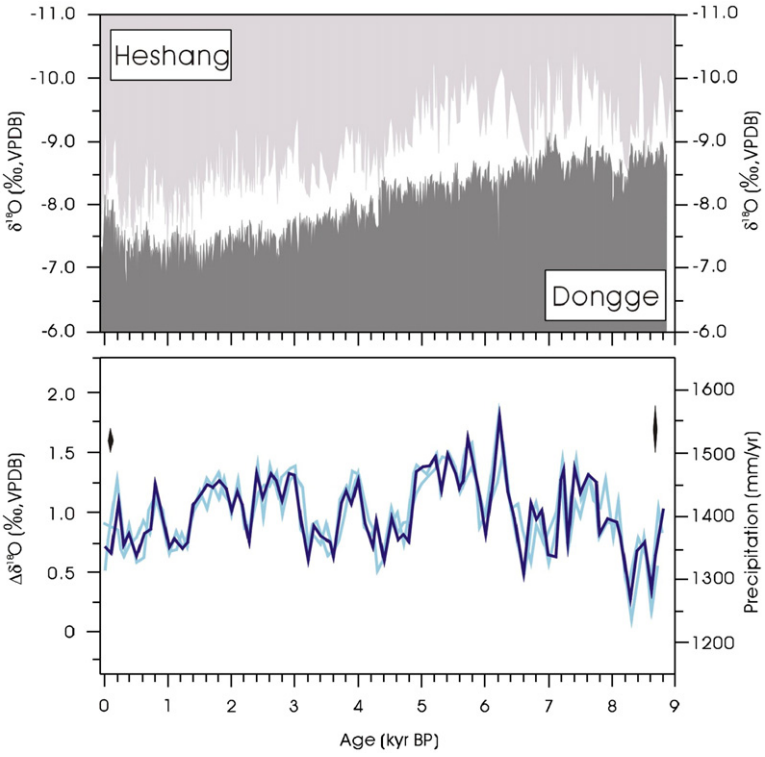

Fig. 7. The measured $\delta^{18}O$ records from Heshang and Dongge (upper panel), together with $\Delta\delta^{18}O$ (=the difference between the two records) and reconstructed past rainfall based on the relationship in Fig. 9 (lower panel). Note the inverted scale in the upper panel, and that Heshang is always more depleted than Dongge. The solid blue line in the lower panel is $\Delta\delta^{18}O$. This is calculated by differencing a 100 yrs average for both records. With typical age uncertainty of ±67 yrs, this averaging process encompasses the age uncertainty. To further assess the effect of age uncertainty, the Dongge record is shifted 50 yrs young, and 50 yrs old, and $\Delta\delta^{18}O$ recalculated, as shown by the two faint blue lines. This analysis demonstrates that the $\Delta\delta^{18}O$ record is robust to age uncertainty. Analytical uncertainty in $\Delta\delta^{18}O$ is ≈0.15‰ based on combination of the errors on analyses in the two caves and is shown by the bar on the top left of the figure. The bar on the top right also encompasses uncertainty due to scatter about the linear relationship shown in Fig. 9. (For interpretation of the references to colour in this figure legend, the reader is referred to the web version of this article.)

sites is quite similar but Heshang is slightly lower (and hence would be expected to have a higher $\delta^{18}O$) so altitude differences also cannot explain the observed difference. This systematic difference in $\delta^{18}O$ between the two sites therefore appears to be controlled by the amount of rain falling between them, potentially providing a quantitative Holocene rainfall history for SW China.

Quantifying rainfall using $\delta^{18}O$ at these two sites assumes that the dominant annual moisture transport has remained similar to that seen today. Several arguments suggest this to be the case, at least for the Holocene. The geography of the region (e.g. coast lines and the Himalayan massif) exerts a strong control on the pattern of winds and has not changed during the Holocene. Analysis of inter-annual variation in moisture transport during the instrumental record from 1952 to 2001 also indicate a uniform moisture transport pathway (Fig. 8). Perhaps most convincingly, a constant moisture trajectory is indicated by numerous GCM simulations of the Asian monsoon at 6 ka (Joussaume, 1999; Braconnot et al., 2002; deNoblet et al., 1996; Bush, 2002). The monsoon circulation is primarily driven by the land-sea thermal contrast, which was higher during the mid-Holocene. Joussaume et al. (1999) report that 18 different model simulations for 6 ka all indicate enhanced low-level convergence into the monsoon low over Eurasia, with the summer monsoon flow extending further inland at this time. While there are differences in model sensitivity, the general pattern is similar in all models, with most atmospheric variables exhibiting only small anomalies relative to the modern. The most significant differences are an increased meridional component of the low-level circulation at 6 ka manifested as northward shifts in monsoon rainfall (Braconnot et al., 2002; deNoblet et al., 1996). These models therefore suggest that any circulation changes were small and parallel with the modern trajectories, so use of the two-site $\delta^{18}O$ approach appears appropriate in this setting.

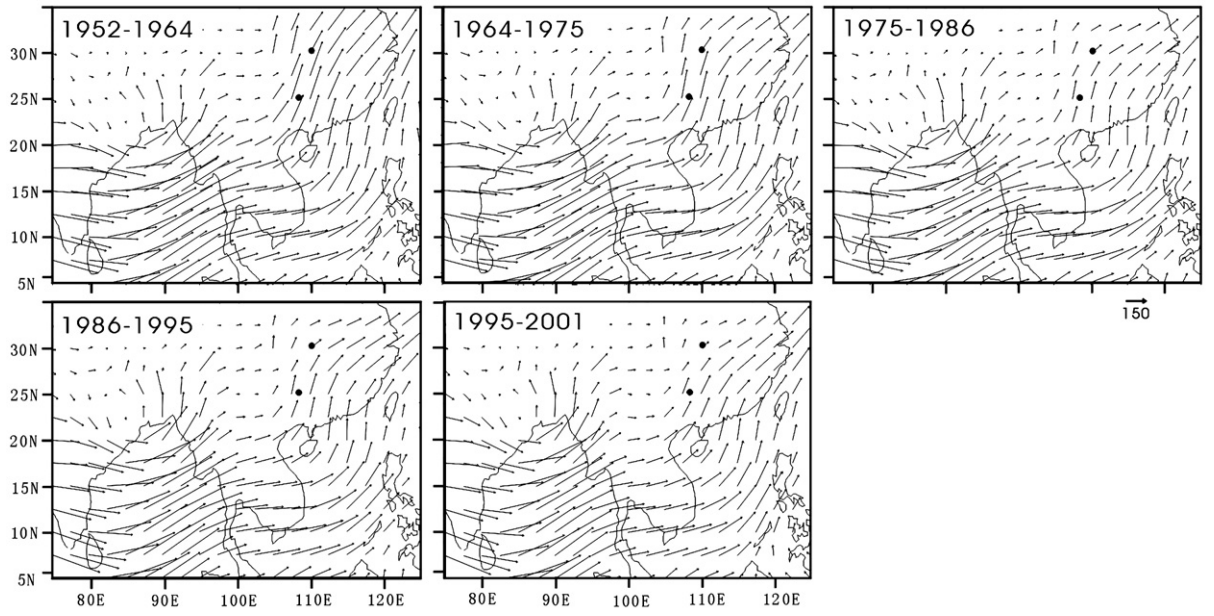

Fig. 8. Average atmospheric moisture transport vectors for summer months, for periods equivalent to the five time-slices shown in Fig. 9. The arrow in the bottom right gives the scale, with units of kg m^{-1} s^{-1}. These values are based on reanalysis of modern atmospheric measurements and are derived by multiplying humidity (kg/m^3) by wind speed (m/s) and summing over the whole air column. Note that the moisture transport direction between the two caves remains constant with time.

5.3. A quantitative history of Holocene rainfall for SW China

The difference between $\delta^{18}O$ at Dongge and Heshang ($\Delta\delta^{18}O$) can be calibrated to rainfall using the instrumental record of the last 54 yrs. Five $\delta^{18}O$ samples from Dongge with an average resolution of 9 yrs are compared with averages of annual samples from the same period from Heshang to yield approximately decadal values for $\Delta\delta^{18}O$ (Fig. 4). These values are compared with the average rainfall between the two caves for each time-period based on the six rainfall stations (Fig. 1). As expected if rainfall is the dominant control on $\Delta\delta^{18}O$ a strong relationship is observed (Fig. 9). In addition to supporting the use of the two-site approach, this relationship also allows a scaling of $\Delta\delta^{18}O$ to average annual rainfall which incorporates uncertainty due to winter rainfall or continental water recycling. Decadal average values of $\Delta\delta^{18}O$ span a range of 0.7 and capture most of the variation seen during the Holocene so that little extrapolation beyond this calibrated range is required.

Assessment of uncertainty in this calibration involves both analytical uncertainty in $\Delta\delta^{18}O$, and uncertainty in the rainfall to $\Delta\delta^{18}O$ relationship. We assess $\Delta\delta^{18}O$ error as the quadratic sum of measurement of a single $\delta^{18}O$ value at the two sites. This is a conservative estimate of error because $\Delta\delta^{18}O$ calculation averages many individual $\delta^{18}O$ values. We assume that the uncertainty in conversion of $\Delta\delta^{18}O$ to rainfall is represented by the scatter about their co-relation during the period of the instrumental record (Fig. 9). This assumes that the instrumental record is long enough to assess uncertainty,

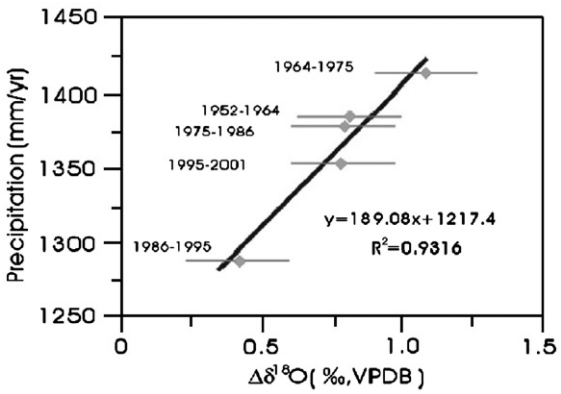

Fig. 9. Comparison of instrumental rainfall records from the last 50 yrs with $\Delta\delta^{18}O$. Age ranges for each datapoint reflect those captured by sampling intervals in the Dongge record (Wang et al., 2005). Rainfall data is the average annual rainfall at the six stations shown in Fig. 1 in mm/yr. As expected, larger differences between $\delta^{18}O$ at the two caves relates to higher annual rainfall. The observed relationship is not a simple Rayleigh Fractionation due to the effects of local terrestrial recycling of moisture (Brubaker et al., 1993; Ingraham and Taylor, 1991).

and that it incorporates any variability due to slight changes in moisture transport pathway or water-recycling. These are reasonable assumptions, although their robustness cannot be further tested with the available data. Future modelling work may help to provide additional quantification of the errors associated with the conversion of $\Delta\delta^{18}O$ to rainfall.

We use the relationship with rainfall to convert measured $\Delta\delta^{18}O$ into a quantitative reconstruction of rainfall in the region between Dongge and Heshang during the Holocene (Fig. 7). This region, although representing only a portion of the total area influenced by the Asian monsoon, is nevertheless representative of the East Asian monsoon, and has particular significance because it lies in SW China, close to the Yangtze river and regions of significant flooding in years of unusually strong monsoon rainfall.

The record of southwest-China rainfall indicates that rainfall was 3% higher than modern in the period 8.2–6.4 ka, 8% higher than modern during between 6.4 and 5.0 ka, and 4% higher during the period 5.0–3.0 ka. Higher rainfall than present throughout the Holocene agrees with the qualitative interpretation of $\delta^{18}O$ records from either Dongge or Heshang and is expected based on higher northern hemisphere insolation driving stronger continental heating. But in other ways the $\Delta\delta^{18}O$ record differs from individual records. In both of the individual records there is little change in $\delta^{18}O$ between ≈8 ka and ≈5 ka, suggesting uniform strong rainfall during the early Holocene. But $\Delta\delta^{18}O$ indicates lower rainfall during the period 8.2–6.4 ka, with an increase after 6.4 ka. This difference may reflect a change in the $\delta^{18}O$ and location of the source of moisture which influenced $\delta^{18}O$ at both locations but not the difference between them. Sea-level was still increasing slowly during the early Holocene following deglaciation, leading to small changes in the $\delta^{18}O$ of seawater and changes in coastlines in Indonesia and elsewhere. Alternatively, the difference between regional and single-site rainfall reconstructions might reflect significantly higher rainfall upwind of Dongge (decreasing $\delta^{18}O$ before it reaches Dongge).

At multi-centennial timescales, the Heshang record shows significantly more variability than the Dongge record. Larger variability of the more inland site is well explained by rainfall-induced $\delta^{18}O$ change between the two sites and argues against a change in overall atmospheric circulation which would be expected to influence both records together. This adds confidence to the interpretation of dry and wet multi-centennial events in the $\Delta\delta^{18}O$ record. The most pronounced dry event occurs at 8.25 ka when rainfall is 7% lower than present, and 14% lower than that at ≈6 ka. This event is likely to be correlative with the 8.2 ka event first observed in the North Atlantic region (Alley and Agustsdottir, 2005). Weakening of the monsoon during cooling in the northern hemisphere at this time mirrors the relationship seen during millennial events of MIS 3 at Hulu Cave (Wang et al., 2001) and may be related to changing ITCZ position caused by this Northern Hemisphere cooling e.g. (Chiang and Bitz, 2005). A lower-amplitude millennial cold period around the abrupt 8.2 ka event has been noted in Greenland ice-core records (Alley and Agustsdottir, 2005; Rohling and Palikie, 2005). The slightly early onset and longer duration of the event in the southwest China rainfall record (and in the $\delta^{13}C$ record from HS-4) may suggest some influence of this longer cold period in the monsoon, although the duration, nature and timing of the abrupt 8.2 ka event in the north Atlantic region is still a matter of some debate (Ellison et al., 2006).

Other millennial to centennial periods of monsoon weakening in the $\Delta\delta^{18}O$ record are of lower amplitude, but are clearly resolved, particularly at 4.8–4.1 ka, 3.7–3.1 ka, and 1.4–1.0 ka. The same pattern of events is not seen clearly in Holocene records from other areas e.g. (Mayewski et al., 2004). The first of these events has the longest duration and has been recognized in previous lake and pollen records from China (e.g. Morrill et al., 2003 and refs therein). This event is not clearly correlative with any event in the North Atlantic region, but a similar dry period is seen in other regions impacted by the Asian monsoon. This event correlates with the 4.2 ka event that may have led to collapse of the Akkadian empire in Mesopotamia (Cullen et al., 2000) and the Neolithic culture of China (Wu and Liu, 2004).

Multicentennial scale variations in rainfall continue until the present, including a wet and dry period that correlate with the Medieval Warm Period and the Little Ice Age respectively. Above average rainfall is seen for the period 1000AD to 1250AD (correlating with the Medieval Warm Period — a period of relative warmth in the Northern hemisphere Moberg et al., 2005) and below average rainfall in the period 1250AD to 1750 (correlating with the cool European conditions of the Little Ice Age). The sense of change is the same as that seen for other abrupt changes in monsoon strength (i.e. cold North Atlantic with dry Asia), and is again consistent with an atmospheric teleconnection, such as control of the ITCZ position by Northern Hemisphere temperature (Chiang and Bitz, 2005).

5.4. Implications for future work

The recognition and quantification of changing Holocene rainfall in southwest China demonstrates the

power of combining spatially-separated stalagmite $\delta^{18}O$ records to provide information that neither record delivers on its own. The resulting rainfall record, for a continental interior influenced by a major climate system, provides a good target with which to test and refine climate models, and helps to assess the expected magnitude of change in future rainfall in this area.

The use of Dongge and Heshang caves for the Holocene period represents perhaps a best-case scenario for the combination of spatially separated $\delta^{18}O$ records. Both records are high resolution with precise U/Th-based age models and they are situated on a single moisture transport pathway which is expected to be invariant during the period of study. The simple differencing of two sites might also be applied in other areas but in many settings the situation is likely to be more complicated. In such settings, however, inter-comparison of stalagmite $\delta^{18}O$ could be performed using GCM models which capture aspects of the processes controlling atmospheric $\delta^{18}O$ fractionation, and the transport of moisture in the atmosphere e.g. (Schmidt et al., 2005; Sturm et al., 2005). Coupled with such models, the approach described in this paper could be extended to include $\delta^{18}O$ from more than two sites, and could provide quantitative reconstruction of past rainfall in many regions, allowing better understanding of natural rainfall variability and its response in varied climate states.

6. Conclusions

The difference in $\delta^{18}O$ between two stalagmite records from SW China provides a reconstruction of Holocene rainfall in this region. The use of two records removes the effects of secondary controls on $\delta^{18}O$ so that the dominant control becomes regional rainfall. This approach should be applicable in other settings and periods, and might be improved by appropriate atmospheric modelling. In this study it has been used to demonstrate that rainfall in SW China was 8% higher than present at the Holocene optimum, but only 3% higher in the early Holocene. It also indicates pronounced multi-centennial dry periods at $\approx$8.2 ka, 4.5 ka, and during the Little Ice Age. The long term and multi-centennial record of rainfall provides a good target with which to test atmospheric models and indicates the teleconnection of monsoon dry periods to cold periods in the north Atlantic.

Acknowledgements

This work was supported by NSFC Grants 40531004 and 40525008, NERC grant NE/B503925/1 and by the Gary Comer Abrupt Climate Change Fellowship.

References

Alley, R.B., Agustsdottir, A.M., 2005. The 8k event: cause and consequences of a major Holocene abrupt climate change. Quat. Sci. Rev. 24, 1123–1149.

Bar-Matthews, M., Ayalon, A., Kaufman, A., Wasserburg, G.J., 1999. The eastern Mediterranean paleoclimate as a reflection of regional events: Soreq cave, Israel. Earth Planet. Sci. Lett. 166, 85–95.

Bowen, G.J., Revenaugh, J., 2003. Interpolating the isotopic composition of modern meteoric precipitation. Water Resour. Res. 39.

Braconnot, P., Loutre, M.F., Dong, B., Joussaume, S., Valdes, P., Grps, P.P., 2002. How the simulated change in monsoon at 6 ka BP is related to the simulation of the modern climate: results from the Paleoclimate Modeling Intercomparison Project. Clim. Dyn. 19, 107–121.

Brubaker, K.L., Entekhabi, D., Eagleson, P.S., 1993. Estimation of continental precipitation recycling. J. Clim. 6, 1077–1089.

Burns, S.J., Fleitmann, D., Matter, A., Kramers, J., A.-S. A.A., 2003. Indian Ocean climate and an absolute chronology over Dansgaard/Oeshger Events 9 to 13. Science 301, 1365–1367.

Bush, A.B.G., 2002. A comparison of simulated monsoon circulations and snow accumulation in Asia during the mid-Holocene and at the Last Glacial Maximum. Glob. Planet. Change 32, 331–347.

Cheng, H., Edwards, R.L., Hoff, J., Gallup, C.D., Richards, D.A., Asmerom, Y., 2000. The half lives of uranium-234 and thorium-230. Chem. Geol. 169, 17–33.

Chiang, J.C.H., Bitz, C.M., 2005. Influence of high latitude ice cover on the marine Intertropical Convergence Zone. Clim. Dyn. 25, 477–496.

Cullen, H.M., deMenocal, P.B., Hemming, S., Hemming, G., Brown, F.H., Guilderson, T., Sirocko, F., 2000. Climate change and the collapse of the Akkadian empire: evidence from the deep sea. Geology 28, 379–382.

Dansgaard, W., 1964. Stable isotopes in precipitation. Tellus 16, 436–438.

deNoblet, N., Braconnot, P., Joussaume, S., Mason, V., 1996. Sensitivity of simulated Asian and African summer monsoons to orbitally induced variations in insolation 126, 115, and 6 ka BP. Clim. Dyn. 12, 589–603.

Ding, Y., Li, C., Liu, Y., 2004. Overview of the South China Sea Monsoon experiment. Adv. Atmos. Sci. 21, 343–360.

Dykoski, C.A., Edwards, R.L., Cheng, H., Yuan, D.X., Cai, Y.J., Zhang, M.L., Lin, Y.S., Qing, J.M., An, Z.S., Revenaugh, J., 2005. A high-resolution, absolute-dated Holocene and deglacial Asian monsoon record from Dongge Cave, China. Earth Planet. Sci. Lett. 233, 71–86.

Ellison, C.R.W., Chapman, M.R., Hall, I.R., 2006. Surface and deep ocean interactions during the cold climate event 8200 years ago. Science 312, 1929–1932 %R 10.1126/science.1127213.

Fleitmann, D., Burns, S.J., Mudelsee, M., Neff, U., Kramers, J., Mangini, A., Matter, A., 2003. Holocene forcing of the Indian Monsoon recorded in a stalagmite from Southern Oman. Science 300, 1737–1739.

Hendy, C.H., 1971. The isotopic geochemistry of speleothems. Part 1. The calculation of the effects of different modes of formation on the isotopic composition of speleothems and their applicability as paleoclimatic indicators. Geochim. Cosmochim. Acta 35, 805–824.

Hu, C., Huang, J., Fang, N., Xie, S., Henderson, G.M., Cai, Y., 2005. Dissolved Si in salagmite carbonate as a proxy for past rainfall. Geochim. Cosmochim. Acta 69, 2285–2292.

Ingraham, N.L., Taylor, B.E., 1991. Light stable isotope systematics of large-scale hydrologic regimes in California and Nevada. Water Resour. Res. 27, 77–90.

IPCC, 2007. Fourth Assessment Report Summary for Policy Makers.

Johnson, K.R., Ingram, B.L., 2004. Spatial and temporal variability in the stable isotope systematics of modern precipitation in China:

implications for palaeoclimate reconstuctions. Earth Planet. Sci. Lett. 220, 365–378.

Johnson, K.R., Hu, C.Y., Belshaw, N.S., Henderson, G.M., 2006. Seasonal trace element and stable isotope variations in a Chinese speleothem: the potential for high-resolution paleomonsoon reconstruction. Earth Planet. Sci. Lett. 244, 394–407.

Joussaume, S., 1999. a. authors, Monsoon changes for 6000 years ago: results of 18 simulations from the Paleoclimate Modeling Intercomparison Project (PMIP). Geophys. Res. Lett. 26, 859–862.

Kim, S.T., O'Neil, J.R., 1997. Equilibrium and non-equlibrium oxygen isotope effects in synthetic carbonates. Geochim. Cosmochim. Acta 61, 3461–3475.

Mayewski, P.A., Rohling, E.E., Stager, J.C., Karlen, W., Maasch, K.A., Meeker, L.D., Meyerson, E.A., Gasse, F., van Kreveld, S., Holmgren, K., Lee-Thorp, J., Rosqvist, G., Rack, F., Staubwasser, M., Schneider, R.R., Steig, E.J., 2004. Holocene climate variability. Quat. Res. 62, 243–255.

McDermott, F., 2004. Palaeo-climate reconstruction from stable isotope variations in speleothems: a review. Quat. Sci. Rev. 23, 901–918.

Moberg, A., Sonechkin, D.M., Holmgren, K., Datsenko, N.M., Karlen, W., 2005. Highly variable Northern Hemisphere temperatures reconstructed from low- and high-resolution proxy data. Nature 433, 613–617.

Morrill, C., Overpeck, J., Cole, J.E., 2003. A synthesis of abrupt changes in the Asian summer monsoon since the last deglaciation. Holocene 13, 465–476.

Robinson, L.F., Henderson, G.M., Slowey, N.C., 2002. U–Th dating of marine isotope stage 7 in Bahamas slope sediments. Earth Planet. Sci. Lett. 196, 175–187.

Rohling, E.J., Palikie, H., 2005. Centennial-scale climate cooling with a sudden cold event around 8,200 years ago. Nature 434, 975–979.

Schmidt, G.A., Hoffmann, G., Shindell, D.T., Hu, Y.Y., 2005. Modeling atmospheric stable water isotopes and the potential for constraining cloud processes and stratosphere–troposphere water exchange. J. Geophys. Res. Atmos. 110.

Sturm, K., Hoffmann, G., Langmann, B., Stichler, W., 2005. Simulation of delta O-18 in precipitation by the regional circulation model REMOiso. Hydrol. Process. 19, 3425–3444.

Wang, B., 2002. LinHo, rainy season of the Asian-Pacific summer monsoon. J. Clim. 15, 386–398.

Wu, W.X., Liu, T.S., 2004. Possible role of the "Holocene Event 3" on the collapse of neolithic cultures around the Central Plain of China. Quat. Int. 117, 153–166.

Wang, Y.L., Cheng, H., Edwards, R.L., Zn, Z.S., WU, J.Y., Shen, C.C., Dorale, J.A., 2001. A high-resolution absolute-dated late Pleistocene monsoon record from Hulu Cave, China. Science 294, 2345–2348.

Wang, X., Auler, A.S., Edwards, R.L., Cheng, H., Cristalli, P.S., Smart, P.L., Richard, D.A., Shen, C.C., 2004. Wet periods in northeastern Brazil over the past 210 kyr linked to distant climate anomolies. Nature 432, 740–744.

Wang, Y.J., Cheng, H., Edwards, R.L., He, Y.Q., Kong, X.G., An, Z.S., Wu, J.Y., Kelly, M.J., Dykoski, C.A., Li, X.D., 2005. The Holocene Asian monsoon: links to solar changes and North Atlantic climate. Science 308, 854–857.